A METHODOLOGY OF UTILIZING ELECTRIC VEHICLES TO IMPROVE THE RELIABILITY AND RESILIENCY OF THE POWER SYSTEM IN EXTREME WEATHER

A Thesis

by

JUNG KYO JUNG

Submitted to the Graduate and Professional School of
Texas A&M University
in partial fulfillment of the requirements for the degree of

MASTER OF SCIENCE

Chair of Committee,	Thomas J. Overbye
Committee Members,	Adam Birchfield
	Jeyavijayan Rajendran
	S. Camille Peres
Head of Department,	Miroslav M. Begovic

August 2023

Major Subject: Electrical and Computer Engineering

ABSTRACT

In the thesis, a new methodology is presented to investigate the impact of electric vehicles on the power system. The goal is to assess the benefits of using electric vehicles as a power source to enhance the grid's reliability and resilience during extreme weather conditions. The proposed methodology involves modeling electric vehicle charging load and discharging capacity in time series data obtained from the travel demand model in Texas A&M Transportation Institute, mapping electric vehicle charging load and discharging capacity to the power system, and simulating and solving the optimal power flow in Powerworld with extreme weather situations. The research focuses on the case study of the winter storm Uri, which occurred in February 2021 in Texas, affecting a significant part of the United States. The studied grid is a synthetic 7000-bus electric grid on the Texas footprint to mimic the Electric Reliability Council of Texas system without revealing any confidential data. The result demonstrates that utilizing electric vehicles as a power source can help avoid power outages as well as the necessity of load shedding in extreme weather cases.

ACKNOWLEDGMENTS

I would like to express my heartfelt appreciation to Professor Thomas J. Overbye, my academic advisor, for his invaluable guidance and academic support throughout all stages of my research. I would also like to extend my gratitude to my family and friends for their unwavering support and encouraging words during this academic pursuit. Thanks to their support, I am able to receive my Master of Science degree.

CONTRIBUTORS AND FUNDING SOURCES

Contributors

This work was supported by a thesis committee consisting of Professor Thomas J. Overbye [advisor], Professor Adam Birchfield, Jeyavijayan Rajendran of the Department of Electrical & Computer Engineering, and Professor S. Camile Peres of the Department of Public Health Department.

The data related to electric vehicle charging demand was provided by Texas A&M Transportation Institute. The mapping algorithm was developed by Professor Thomas Overbye from the Department of Electrical and Computer Engineering. All other work conducted for the thesis was completed independently by the student.

Funding Sources

The graduate study received substantial funding from the Korea Electric Power Corporation (KEPCO). Additionally, partial support was provided through funding from various sources, including the U.S. National Science Foundation (NSF) under Award 1916142, the U.S. Department of Energy (DOE) under Award DE-OE0000895, and the US ARPA-E Grant No. DE-AR0001366, and the Power Systems Engineering Research Center (PSERC).

NOMENCLATURE

EIA	Energy Information Administration
EVs	Electric Vehicles
ERCOT	Electric Reliability Council of Texas
FERC	Federal Energy Regulatory Commission
ESS	Energy Storage System
LIB	Lithium-ion Battery
LD	Light-Duty
V2G	Vehicle-to-Grid
EPRI	Electric Power Research Institute
TDM	Travel Demand Model
TTI	Texas A&M Transportation Institute
UC	Unit Commitment
OPF	Optimal Power Flow
KCL	Kirchhoff's Current Law
MILP	Mixed-Integer Linear Programming
DC-OPF	Direct Current Optimal Power
AC-OPF	Alternating Current Optimal Power Flow
BNSM	Bayesian Network Statistic Model
CEII	Critical Energy/Electric Infrastructure Information
GDV	Geographical Data View
P.U	Per Unit
SCOPF	Security-Constrained Optimal Power Flow

TABLE OF CONTENTS

Page

LIST OF FIGURES

FIGURE Page

LIST OF TABLES

TABLE Page

1. INTRODUCTION

1.1 Motivation

According to a report from the EIA [1], in 2020, electricity users in the United States experienced over eight hours of power interruptions on average. This is the highest recorded figure since the commencement of data collection on electricity dependability in 2013. Power interruptions can arise due to various factors, such as weather, vegetation growth patterns, and the practices of utility companies. As depicted in Figure 1.1, the duration of power interruptions during major events, such as snowstorms, wildfires, and hurricanes, is considerably longer than without major events.

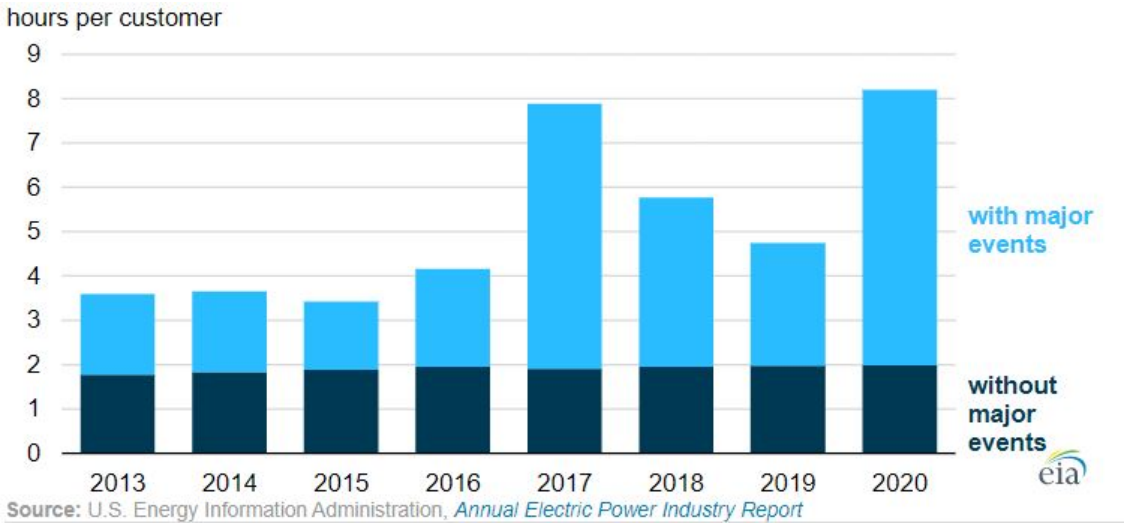

Figure 1.1: U.S. average duration of total annual electric power interruptions (2013-2020) [1].

For example, the Texas winter storm Uri, which occurred on February 15-17, 2021, caused extensive damage to the ERCOT and affected hundreds of thousands of customers. The unexpected low temperatures during the storm led to a surge in demand for heating, putting a strain on the electrical grid. According to the FERC report [7], some generator turbines froze, and there was a

shortage of natural gas reserves, resulting in a generation outage of 41,400MW. To prevent a complete blackout of the ERCOT grid and maintain the optimization problem solvable, load shedding of 10,500MW was necessary. Figure 1.2 shows the impact of the winter storm on system frequency between 1 am and 2 am on Feb 15, 2021. This frequency disturbance was a contributing factor to the need for load shedding.

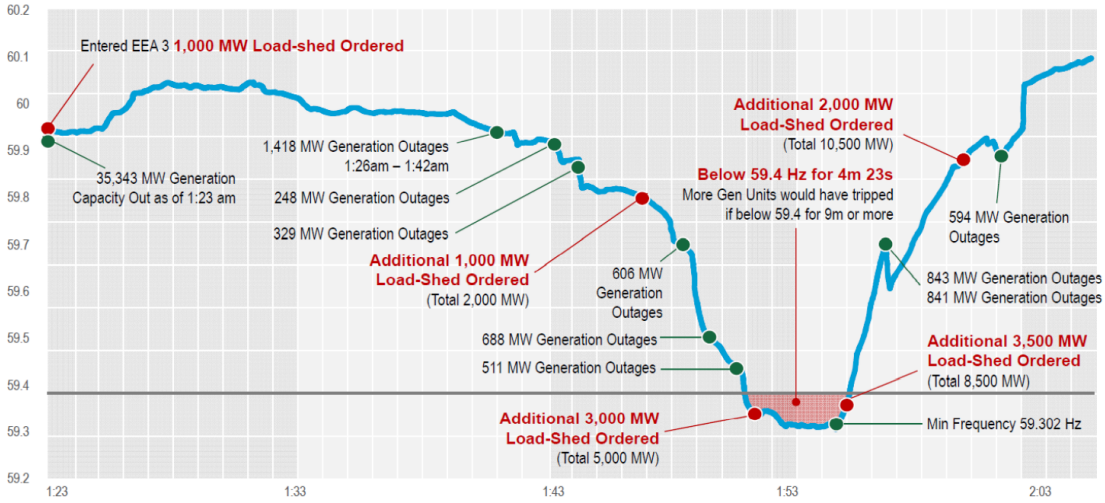

Figure 1.2: The ERCOT grid frequency on the morning of February 15, 2021 [2].

In order to maintain a stable power system, it is crucial to ensure that there is enough generation capacity to meet the demand and losses at all times. Failure to do so can result in a drop in system frequency, which can ultimately lead to voltage collapse and even a blackout of the entire system. To prevent this situation, load shedding may be necessary for situations where the available generation capacity is insufficient or the line capacities are unable to handle the required power transfer. Ensuring a reliable and resilient power grid, particularly in extreme weather events, is a top priority for power system operators and planners. However, severe weather events can pose significant challenges to the power system, as they can disrupt the normal load and operation conditions.

Although ESS is one potential solution to this problem, its installation costs can be prohibitively

expensive. As shown in Figure 1.3, a 60-MW ESS with a 2-hour duration costs $857 per kW, resulting in a total cost of $51,400,000 as calculated in Table (1.1). To prevent load shedding of 10,500 MW, as illustrated in Figure 1.2, the cost of an ESS would be a staggering $8,995,000,000 from Table (1.1) .

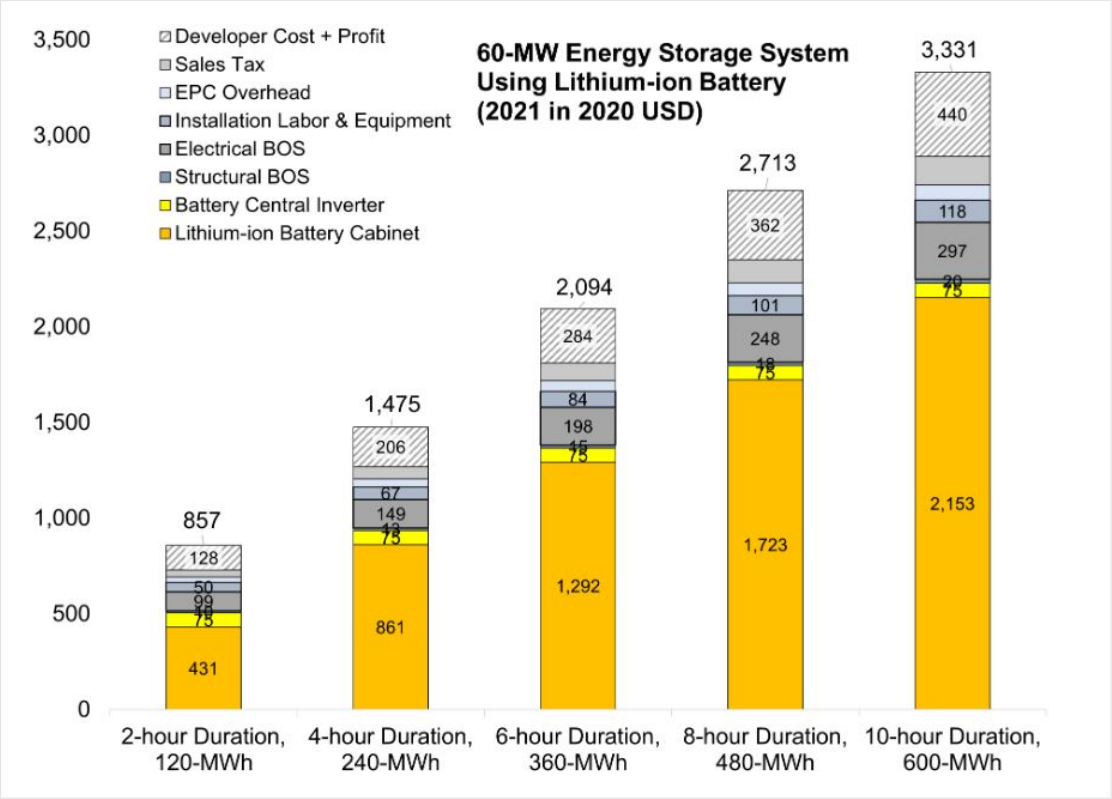

Figure 1.3: 2021 U.S. LIB storage costs for durations of 2-10 hours in $/kW [3].

Utilizing EV batteries as a power source for the grid is another viable solution. According to a 2020 report by Canalys [4], global EV sales reached 3.1 million units, marking a 39% increase from the previous year. This trend is expected to continue, with projected sales of 30 million EVs by 2028, and EVs predicted to account for nearly 50% of new passenger car sales by 2030. Despite the challenges faced by the global passenger car industry in 2020, as shown in Figure 1.4, EVs have become increasingly popular [4]. Additionally, the White House has announced a target for 50%

Table 1.1: U.S. LIB storage costs.

Type	ESS-Size (kW)	ESS-Cost ($/kW)	Total Costs ($)
ESS-60MWh / 2hours	60,000	857	51,400,000
ESS-10500MW / 2hours	10,500,000	857	8,995,000,000

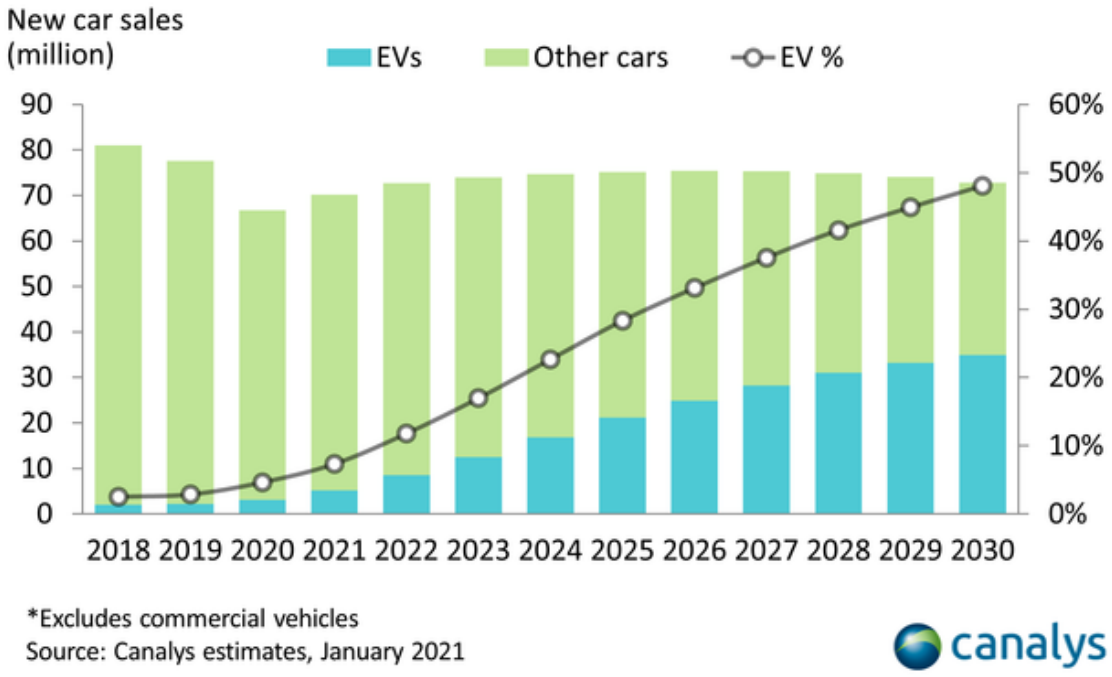

Figure 1.4: Global passenger car sales [4].

market share of light-duty EVs by 2030 in the United States [8].

According to a 2018 system planning report by ERCOT in Texas [6], the penetration of EVs in Texas is projected to reach over 3.2 million by 2033, with the total energy capacity of EV energy storage estimated at approximately 208 GWh based on EV type, including that light-duty EVs (passenger cars) is approximately 60 GWh, Medium-duty EVs (buses) is approximately 28 GWh, and heavy-duty EVs (trucks) is approximately 120 GWh. As shown in Table 1.2, EVs can typically store between 20 and 600 kWh of energy in their batteries. Based on Equation (1.1), the penetration of EVs in Texas is expected to reach 15% by 2033 [9].

Table 1.2: EV penetration in Texas by 2033 from ERCOT report [6].

Type	Number of Vehicles	Per Vehicle Charging (kWh)	Total Energy Capacity (GWh)
Light-duty / Cars	3,000,000	20	60
Medium-duty / Buses	80,000	350	28
Heavy-duty / Trucks	200,000	600	120
Total	3,280,000	20 - 600	208

It is evident that having additional energy storage capacity or EVs capable of injecting power into the grid could have prevented the need for extreme mitigation measures, such as load shedding, during the power failure that occurred in Texas in February 2021. This study aims to explore how EVs can help minimize the impact of power outages in such events.

$$EV\ penetration\ (15\%) = EV(3,280,000)\ /\ Total\ of\ Cars(22,000,000) \tag{1.1}$$

1.2 Review

In general, as renewable resources become more prevalent and are subject to weather fluctuations, coupled with the rise in extreme weather events, largely due to global warming, there is an inclination to rely more on battery storage to enhance the reliability and resilience of the power grid [10]. However, given that energy storage is a relatively expensive power source, it is beneficial to leverage the capabilities of EVs in emergency situations. The bi-directional use of EVs can diminish the need for expensive stationary distributed energy storage.

The utilization of V2G technology as a research field has been proposed for many years to leverage the capacity of EVs as a power source. It can be advantageous to preserve the energy produced by renewable resources in EV batteries and to supply electricity to the grid in case of emergencies [11]. The benefits and drawbacks of the V2G system are discussed in references such as [12]. Reference [13] addresses the technical challenges of bidirectional charging. Furthermore, reference [14] reviews the role of EVs as mobile energy storage devices to improve power system resilience. Both utilities and EV owners can benefit from V2G as demonstrated in reference

[15]. EV owners are remunerated for using the energy stored in their idle vehicles when power transactions are carried out. Reference [16] investigates the effects of V2G on electric grid frequency management, revealing that transient stability has also become a focus in V2G technology, indicating that EVs could potentially provide effective frequency control.

On the other hand, some studies, such as [17], suggest that companies are hesitant to adopt V2G technology due to concerns about reduced battery life and increased driver anxiety about depleting their charge. However, as EV battery technology continues to improve, these issues are becoming less significant. In fact, in 2022, Ford became one of the pioneers in implementing bi-directional EV chargers and launched its own affordable bi-directional home charging station [18]. Furthermore, EPRI has initiated a project to evaluate the feasibility of integrating V2G technology with mainstream car manufacturers such as Fiat Chrysler Automobiles and Honda Motor, both of which offer cars with bidirectional power conversion systems [12].

1.3 Objective

The purpose of this study is to examine the impact of EVs on the grid and demonstrate the benefits of utilizing them as a power source to enhance the reliability and resilience of the power grid in severe weather conditions. The research is based on a case study of the winter storm Uri that occurred in Texas in February 2021, which affected a large area of the United States. To simulate the ERCOT system without revealing confidential data, a synthetic 7000-bus grid on the Texas footprint is used. The study aims to map EV charging load and EV discharging capacity to the existing electric grid using the Voronoi polygons with nodes located centrally within their respective service areas. The results will be used to solve optimal power flow during the 2021 winter storm Uri case with a comparison between the base load case and the EV 15% penetration load case. The objectives of this thesis can be summarized as follows:

- Modeling EV charging load - The data of EV charging load is performed by using the 2020 regional Travel Demand Model from TTI in the Houston and Austin area.
- Mapping EV charging load to Transmission system - the charging load is mapped to the

electrical grid models based on their latitudes, longitudes, and geographical coordinates of substations and buses in the grid by using Voronoi polygons.

- Load Time Series - The geographic coordinates of each bus are used to determine a unique electricity consumption profile at that location. An iterative aggregation approach is taken to integrate publicly available building- and facility-level load time series to the bus level.

- Vehicle to Grid Modeling - The possibility of connecting EVs to the grid is modeled as EV discharging capacity at the end-of-trip locations of EV fleets where the vehicles are parked and in idle mode.

- Simulate and Solve optimal power flow - The hourly required demand to charge EVs in specific locations and times of the day is calculated based on travel patterns and then added to the hourly load of the studied grid over the Texas footprint.

2. BACKGROUND*

2.1 System Elements

Before explaining the proposed methodology to solve OPF in the power system, it is important to define what system elements will be used in the simulations and what purposes they serve. These are the elements used:

- Generators: Maximum generation in the 7000-bus Synthetic grid is 104.9GW. Natural gas generation is 56.5GW, Wind power generation is 25.7GW, Coal power generation is 14.4GW, and Nuclear power generation is 4.7GW. During the Texas winter storm Uri, the maximum generation is 63.5GW at 1 am on February 15, 2021, because some generators were frozen and a shortage of natural gas which is a total of 41.4GW.
- Loads: Maximum loads in the 7000-bus Synthetic grid is 74.7GW. During the Texas winter storm Uri, the highest load is 65.9GW at 1 am in February 15th, 2021.
- Substations: Substations in the 7000-bus Synthetic grid are 4,894.
- Buses: Buses in the 7000-bus Synthetic grid are 6,717.
- EV charging load: the demands are 1.5GW. The transportation data from TTI is distributed 24 hours a day and converted to EV charging load. The demand is assumed to EV 15% penetration by 2033 from the 2018 ERCOT LTSA Report.
- EV discharging capacity: The capacity is 6GW. The transportation data from TTI is distributed 24 hours a day and converted to EV discharging capacity as a power source. The capacity is assumed EV 15% penetration by 2033 from the 2018 ERCOT LTSA Report.

This work proposed a method to simulate EV charging load and discharging capacity in the 7000-bus synthetic grid in Texas and solve for the optimal power flow in steady-state power systems in harsh weather cases. The core of the solution process is the power flow equations that describe the steady-state behavior of the power system.

2.2 Electric System Formulation

2.2.1 Unit Commitment

The problem of UC involves determining whether a power generation unit should operate or not within specific time intervals [19, 20, 21]. In the context of DC-OPF, binary variables have been suggested in the literature to model the on/off status of generation units [22]. Incorporating UC into DC-OPF results in a MILP problem that can be computationally demanding, especially for larger cases, due to the non-linear increase in the size of the optimization problem with the number of variables [23]. In order to incorporate the constraints on reactive power and create a more realistic model, this research proposes the utilization of AC-OPF. Nevertheless, using AC-OPF would cause an increase in the computational cost of the problem, since it is non-linear and non-convex. As the industrial electrical grids are often large in size and voltage/reactive power control settings are included in the problem, including binary variables in the AC-OPF optimization problem would make it NP-Hard and even more computationally demanding [24, 25].

2.2.2 Direct Inclusion of Weather Data

In our previous research [26], we proposed a method for connecting weather stations to electric grid generators. This approach involved integrating time-dependent weather data, such as wind speed, cloud coverage percentage, and temperature, directly into the OPF model to obtain real-time generator capacities, especially for renewable generators, based on the prevailing weather conditions. The renewable generator models were extracted from [27]. These models and input data were then utilized in a time-step simulation to update the actual capacities of generators and determine the output generation of renewable resources based on their availability [26].

2.2.3 Bus Admittance Matrix

In ac circuits, impedance is used in Equation (2.1). The initial step in solving the Power Flow Equation (2.2) is to construct an admittance matrix, commonly known as the Y_{bus}. The Y_{bus} is necessary for power flow calculation, as it forms a crucial part of the relationship between the bus voltages (V) and the bus currents (I) in Equation (2.3). By applying KCL at each bus in the system, the Y_{bus} is derived to establish the relationship between the bus current injections, bus voltages, and branch impedances and admittances.

$$Z = R + jX \tag{2.1}$$

$$Y = \frac{1}{R + jX} = \frac{R}{R^2 + X^2} + j(\frac{-X}{R^2 + X^2}) = G + jB \tag{2.2}$$

$$I = Y_{bus}\, V \tag{2.3}$$

2.2.4 Power Balance Equations

According to KCL, the current injection (I_i) at each bus (i) in an n-bus system must be equivalent to the current flowing into the network. This relationship can be expressed as I = Ybus V, which is used in both Equation (2.4) and Equation (2.5).

$$I_i = I_{Gi} - I_{Di} = \sum_{k=1}^{n} = \; I_{ik} = \; Y_{ik}\, V_k \tag{2.4}$$

$$S_i = V_i\, I_i^* = V_i \sum_{k=1}^{n} Y_{ik}^*\, V_k^* = \sum_{k=1}^{n} |V_i|\,|V_k|(\cos\theta_{ik} + j\sin\theta_{ik})(G_{ik} - jB_{ik}) \tag{2.5}$$

2.2.5 AC-OPF

To determine the steady-state outcomes that minimize the generation cost from Equation (2.6) in a power system, the AC-OPF method, as outlined in [19], is utilized. The coefficients (a, b, and

c) that represent the quadratic cost curve elements of generators are used to define $\mathcal{F}_c(P_G)$:

$$\min_{P_G} \mathcal{F}_c(P_G) = \sum_{g=1}^{|\mathcal{G}|} [a_g + b_g P_{G,g} + c_g P_{G,g}^2] \tag{2.6}$$

In order to maintain a power balance in a system, the power balancing equations, such as Equation (2.7) and Equation (2.8), must be fulfilled. Furthermore, additional operational constraints from Equation (2.9) to Equation (2.12) specified in [19] must also be taken into account.

$$P_{G,(g \in g(i))} - P_{D,i} = |V_i| \sum_{k=1}^{|N|} |V_k| (G_{ik}^Y cos\theta_{ik} + B_{ik}^Y sin\theta_{ik}) \tag{2.7}$$

$$Q_{G,(g \in g(i))} - Q_{D,i} = |V_i| \sum_{k=1}^{|N|} |V_k| (G_{ik}^Y sin\theta_{ik} - B_{ik}^Y cos\theta_{ik}) \tag{2.8}$$

$$P_{min,g} \leq P_{G,g} \leq P_{max,g} \qquad \forall g \in \mathcal{G} \tag{2.9}$$

$$Q_{min,g} \leq Q_{G,g} \leq Q_{max,g} \qquad \forall g \in \mathcal{G} \tag{2.10}$$

$$V_{min,i} \leq |V_i| \leq V_{max,i} \qquad \forall i \in \mathcal{N} \tag{2.11}$$

$$P_e^2 + Q_e^2 \leq S_{max,e}^2 \qquad \forall e \in \mathcal{E} \tag{2.12}$$

The variables $|V_i|$ and $|\theta_i|$ in the equations represent the magnitude and phase angle of the voltage at the i-th bus, respectively. The parameter θ_{ik} denotes the voltage angle difference between the i-th and k-th buses. The system is modeled as a collection of buses, represented by the set N, with real and reactive power demands at the i-th bus denoted as $P_{D,i}$ and $Q_{D,i}$, respectively. The real and reactive power outputs of the g-th generator are represented as $P_{G,g}$ and $Q_{G,g}$, respectively.

The set of all generators in the system is denoted by $\mathcal{G}$. The real and reactive components of the

Y-bus matrix are represented by G_{ik}^{Y} and B_{ik}^{Y}, respectively. The generator operating limits, in terms of real and reactive power, are defined by $(P_{min,g}, P_{max,g})$ and $(Q_{min,g}, Q_{max,g})$, respectively. The bus voltage limits are constrained by $(V_{min,i}, V_{max,i})$. The power flow to each bus e is constrained by the thermal limit $S_{max,e}$, which is connected to the flow of real and reactive power in Equation (2.12). The power flowing into each bus is determined by the power equations in Equation (2.13) and Equation (2.14).

$$P_e = |V_i|^2 G_{ik}^{Y} - |V_i||V_k|(G_{ik}^{Y} cos\theta_{ik} + B_{ik}^{Y} sin\theta_{ik}) \tag{2.13}$$

$$Q_e = -|V_i|^2 B_{ik}^{Y} - |V_i||V_k|(B_{ik}^{Y} cos\theta_{ik} - G_{ik}^{Y} sin\theta_{ik}) \tag{2.14}$$

2.3 Modeling EVs in the Electrical Grid

2.3.1 EV Charging Demand Modeling

The first step of the algorithm involves computing EV charging demands. In the study, such as [28] and [29], they describe and elaborate on various charging scenarios for the integrated modeling of EVs. The spatiotemporal charging demand serves as a bridge between the transportation and electrical grids. To generate a realistic charging pattern, we developed a strategy that incorporates the original travel model for trip origins and destinations, an EV's dynamic model for energy consumption, and surveys on travel and charging behavior. The simulation of EV charging used the TDM and travel studies from [30]. TDM provides information on both the departure and arrival locations (start and end-travel nodes) and also provides data on total distances, operating time, and fuel consumption in the regional transportation network throughout a day in 2020. The network was created using urban traffic simulation techniques [31], and the Mobiliti simulator [32] was employed to generate the traffic dynamics.

The model used in the study predicts the power consumption of EVs during travel by generating travel paths based on inputs such as the transportation system and travel needs. A subset of these paths is randomly selected for EV travel based on a predetermined market share for EVs. To

analyze the impact of different transportation-related factors on energy consumption, an activity-based EV model is utilized. In the next step, a parametric simulation inference technique is used to estimate the power usage of EVs based on their in-transit operation conditions. To describe the powertrain of the vehicle, a BNSM is employed, which utilizes prior industry experience and can be improved using an information-based approach. The modeling and verification of this approach are discussed in detail in [33].

To simulate EV usage in the region, the study used a list of trips and specified a percentage of penetration for various types of EVs, such as those with a 100, 200, or 300-mile range. The range of each EV in the network was chosen based on expected market penetration from EV sales data [34]. Of the overall EV fleet, those with ranges of 100, 200, and 300 miles accounted for 25%, 13%, and 52%, respectively. The model starts by simulating the state of charge of each EV at the beginning of its trip, taking into account the energy usage patterns specific to the EV's range. It then determines whether the EV needs to recharge during the trip based on available energy. If the model predicts that the trip will be the EV's last for the day, it assigns home charging demand accordingly. To estimate the energy usage rate per mile for each driving, the model uses the driving length and velocity information obtained from the travel itineraries and fits it to the EV models. By modeling the recharging needs, the driving in road usage is converted into charging demands. Finally, to account for uncertainties in the model, a Monte Carlo simulation strategy is employed in Equation (2.15). In this equation, $\hat{X}$ represents the estimated value of the variable of interest, which is calculated by taking the average of the function $f(X_i)$ evaluated at each of the N random samples X_i. The Monte Carlo simulation involves generating a large number of random samples from the probability distribution of the uncertain input variables and using these samples to estimate the distribution of the output variable.

$$\hat{X} = \frac{1}{N} \sum_{i=1}^{N} f(X_i) \tag{2.15}$$

2.3.2 Mapping EV Charging Demand to the Electrical Grid

The second step of the algorithm involves mapping EV charging demand onto the electrical grid using a Voronoi diagram. The mathematical concept enables a specific space to be divided into sections based on proximity to a set of input points. Each section in the Voronoi diagram is defined by a set of points that are closer to a specific input point than to any other input point. In more precise terms, the Voronoi diagram can be understood as the aggregation of all Voronoi regions. The Voronoi region for a point s in the set (S) is defined in Equation (2.16). The final Voronoi diagram can be expressed as Equation (2.17).

$$Vor(s) = p : distance(s, p) \leq distance(s', p), \forall s' \in \mathcal{S} \tag{2.16}$$

$$Vor(\mathcal{S}) = \cup_{s \in \mathcal{S}} Vor(s) \tag{2.17}$$

EV charging demand loads are mapped to the electrical grid using Voronoi diagrams, which enable transmission-level mapping to substations. The substation is designated as the seed point, and the Voronoi polygon determines the service area. The location and time series of EV charging demand loads are derived from the results of transportation studies and simulations. To incorporate this information in power system simulation, the geographic coordinates, latitudes, and longitudes of the grid's substations and buses are utilized. The mapping of EV charging demand loads to electric grid substations is detailed in [35].

2.3.3 Load Time Series

In the third step of the algorithm, Load Time Series is created by following the approach outlined in [36] and [37]. The method generates 24-hour time series load data for each bus over a year by considering the load data for each time step and utilizing the physical locations of each bus to develop a unique power usage profile for the region. Next, an iterative aggregation technique is employed to combine freely available building-level and facility-level load time data with the

buses. The process combines the location prototype building and facility load data for each node in the system, including residential, commercial, and industrial loads. To validate the synthetic load data generated at each time step, the time series of an authentic power system in [37] is applied.

After the EV charging demand loads are linked to their corresponding substations in the transmission system, the EV load time series is depicted as loads at the bus level within its designated substations. These newly incorporated loads are also taken into account while updating the synthetic load data at the bus level.

2.3.4 Vehicle to Grid Modeling

In the last step of the algorithm, the focus is on modeling the connection of EVs to the electrical grid by considering them as a power source such as energy storage while they are in idle mode and parked at the end-of-trip locations. The start and end-travel nodes of the travel path are obtained from TDM and if the distance traveled is less than 40 miles, it is assumed that the EVs are not depleted and can serve as a power source. The parking locations of EV fleets are then mapped to the transmission-level substations of the electrical grid model using Voronoi diagrams. EV discharging capacities that are in idle mode are assigned to the substations connected to the end-travel nodes of the EV fleets. These capacities are then integrated into the electrical grid model as generators, such as energy storage.

2.4 Case Study

2.4.1 Grid Model

This study utilized publicly available data to create a synthetic but realistic grid that covers the geographical region of Texas in the United States. To ensure confidentiality and protect CEII, the grid was developed using U.S. Census statistics [38] and EIA data on generators [39]. The grid's creation process, including the assignment of substations, transmission lines, and reactive power control devices, is explained in detail in [40]. The synthetic grid was created and validated using metrics that resemble those of actual grids, providing realistic data sets [41, 42]. Geographical data for system components played a critical role in the creation of these synthetic grids. The synthetic

Table 2.1: Texas synthetic grid statistics.

Parameter	Numerical value
Buses	6,717
Generators	731
Loads	5,095
Switched shunts	634
Substations	4,894
Transmission lines	7,173
Maximum load (MW)	74,667
Maximum generation (MW)	104,914

grid, which covers the ERCOT geographical territory, contains 7000 buses, as shown in Figure 2.1, with 345 kV transmission lines displayed in bold green, 138 kV lines in black, and 69 kV lines in light green [43]. The grid's data set is publicly accessible.

In accordance with the approach introduced in [44, 45], Figure 2.2 illustrates a GDV of the load substations, along with the primary parameters of the scenario and the highest load are presented in Table 2.1. The magnitude of the oval shape corresponds to the size of the power stations.

2.4.2 Transportation Data

We restricted our transportation data to the geographical areas of Austin and Houston in Texas, US, as the data for Dallas was unavailable at the time of the study. Future research will update the simulation with Dallas transportation data for improvement. As indicated in Fig. 2.3, Dallas, Austin, and Houston have the highest number of EV registrations in Texas [46]. In addition, Fig. 2.2 shows that these cities have the highest electricity demand, which is directly related to the population distribution in Texas. Therefore, these cities are prime locations for utilizing EVs as a power source for emergency situations such as the Texas winter storm Uri. The EV charging scenarios were designed to replicate the natural charging patterns of drivers and fleets, and to model the anticipated EV 15% penetration rate by 2033 [6].

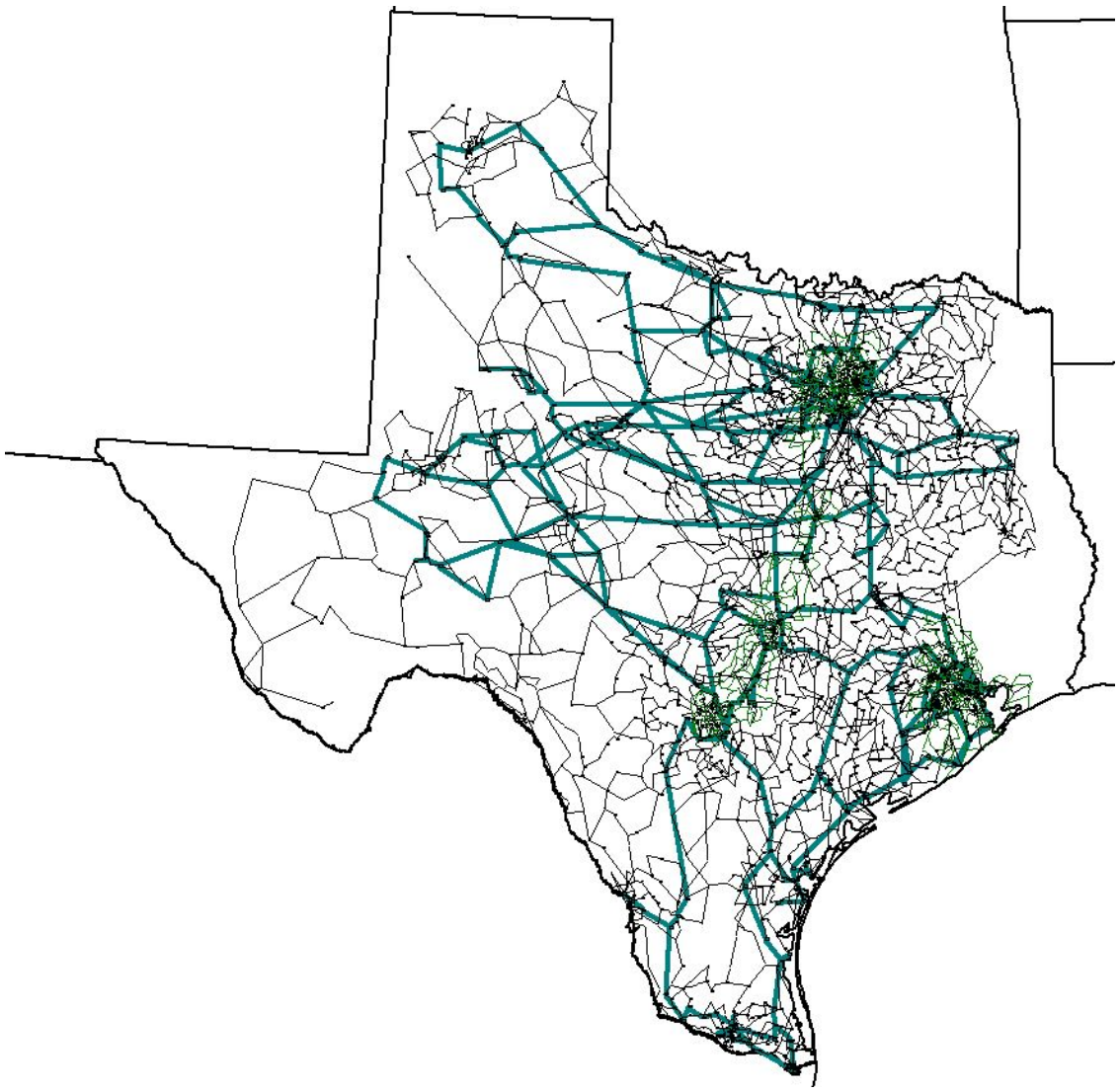

Figure 2.1: The one-line diagram of transmission lines of the studied grid over Texas footprint. Reprinted with permission from [5].

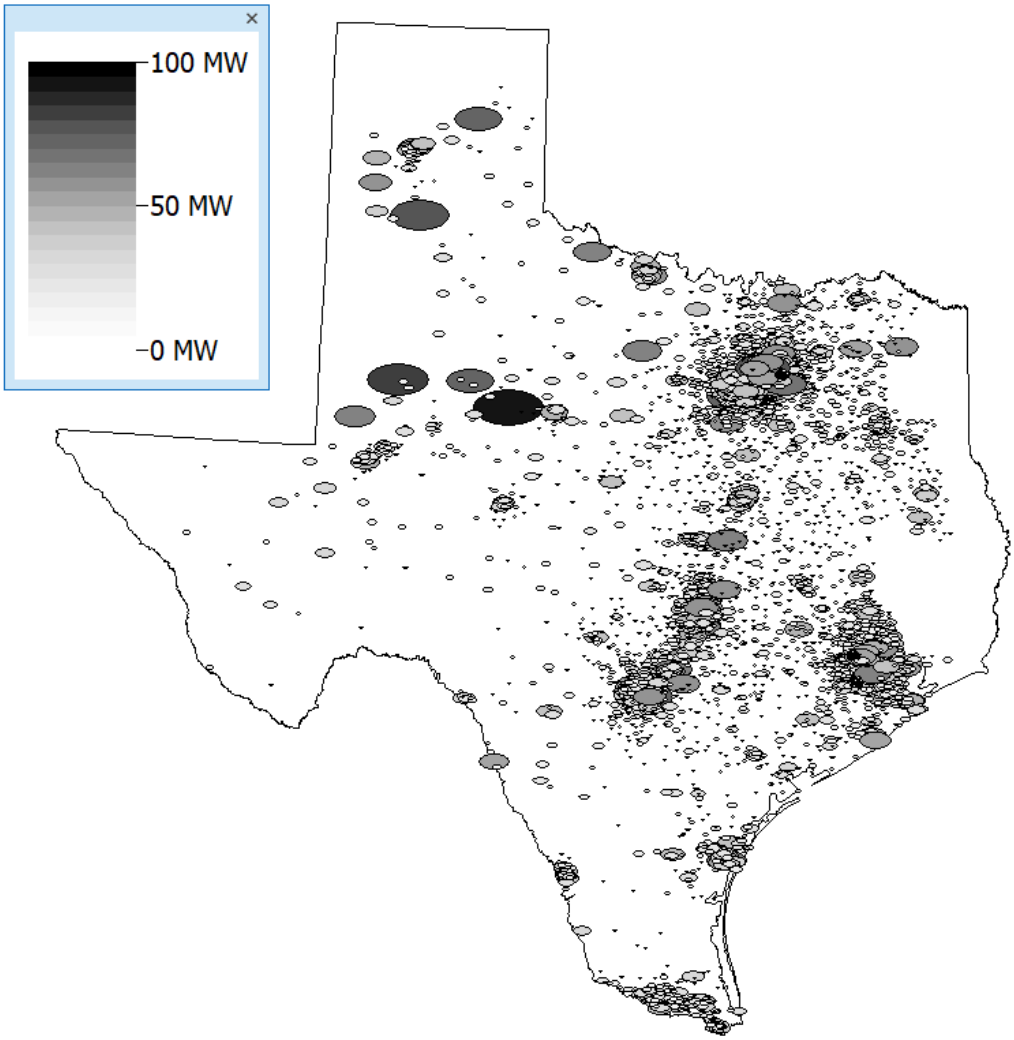

Figure 2.2: Geographical data view of load substations in peak loads in the Texas case study. Reprinted with permission from [5].

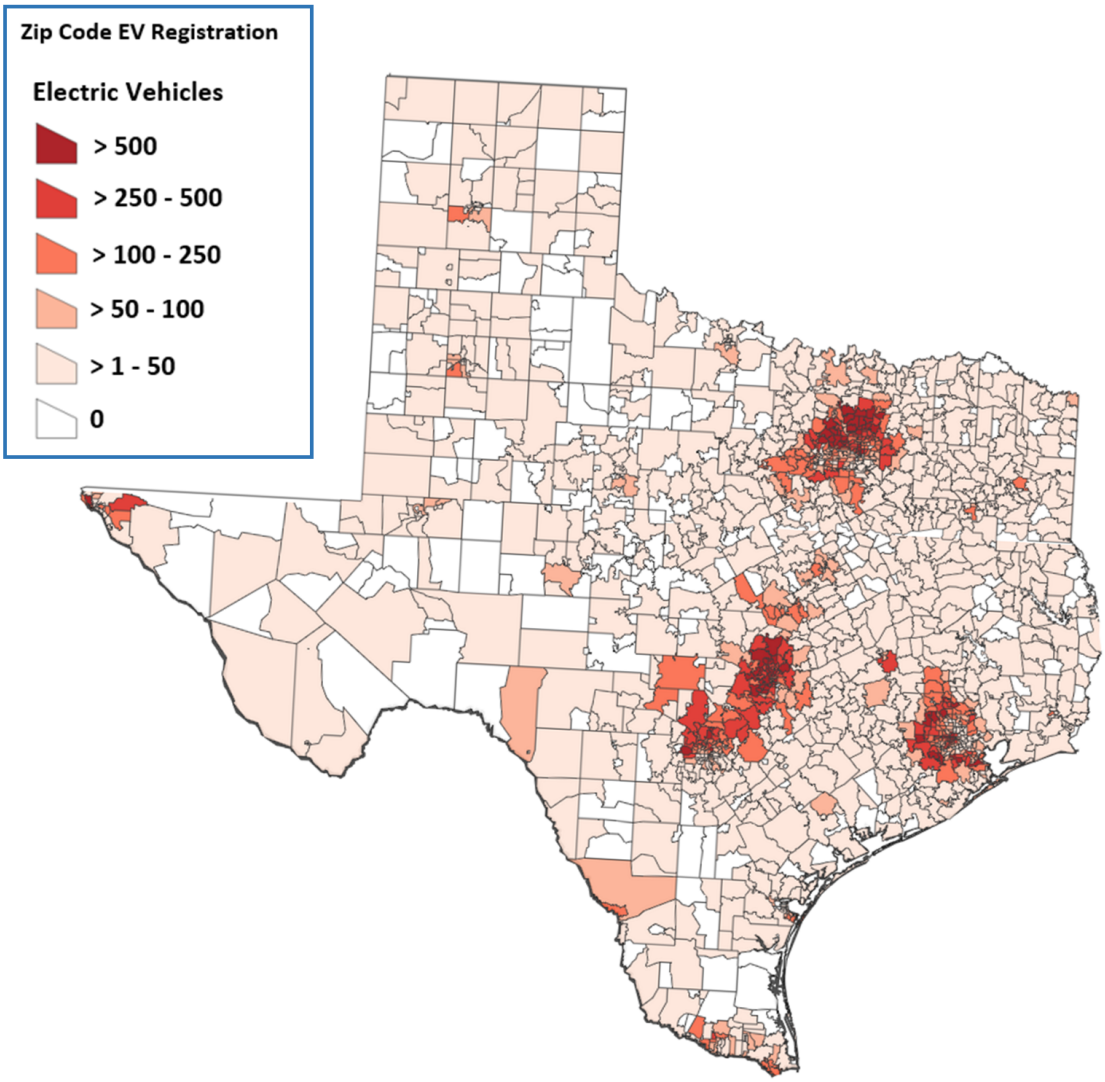

Figure 2.3: Texas electric vehicle registration mapping. Reprinted with permission from [5].

Table 2.2: Two scenarios in the PowerWorld.

Case	Generation	V2G Batteries	Total	Load	V2G Load	Total
The Base Case	63.5GW	-	63.5GW	65.9GW	-	65.9GW
The V2G Case	63.5GW	6.0GW	69.5GW	65.9GW	1.5GW	67.4GW

2.4.3 Simulation Scenarios

The scenarios explored in this study focus on February 15, 2021, and include weather and load data. Hourly load data was generated at the bus level and adjusted based on [7]. The study employed weather models based on [26] and gathered hourly temperature, wind speed, wind direction, cloud coverage percentage, and dew point measurements from Texas weather stations, which were then incorporated into optimal power flow models to update the output and actual capacities of generators, particularly renewable generators.

Two scenarios that are studied in the study in Table 2.2 include :

- The Base case: Texas load on February 15, 2021
- The V2G case: Texas load with the addition of the required EV charging demand with EV 15% penetration as well as V2G discharging capacities

3. SUMMARY AND RESULTS*

3.1 Summary

The simulations in the study were conducted using Powerworld, Python, and MATLAB, which were installed on a machine with an Intel(R) Xeon(R) CPU E5-1650 v4 @ 3.60GHz and 64GB of RAM. In the base case simulation, which incorporated load and weather impacts but did not involve any EVs, the simulation arose a convergence issue due to voltage collapses on February 15, 2021. Specifically, there were low voltage issues below 0.9 p.u in 165 buses in the North of Texas, while high voltage problems above 1.1 p.u were observed in 1747 buses in the West of Texas. Overall, 1912 buses experienced severe voltage violations due to generation shortages compared to the load. In general, if generation is lower than load in a real electrical grid, it would go blackout. However, Powerworld showed only the voltage collapse because the slack bus provided unlimited real and reactive power in the electrical grid. For this reason, to prevent a statewide blackout, ERCOT enforced load shedding several times in this situation.

3.2 Results

Figure 3.1 illustrates a voltage contour map of buses in the case study, based on the voltage strategy proposed in [47]. Notably, since the generation capacities were insufficient to meet the load and loss of the electrical grid, it came to a voltage collapse. However, after implementing the impact of EVs by mapping EV charging load and discharging capacity on the electrical grid, the generation capabilities from EV discharging capacities increased by around 6 GW, offsetting the additional 1.5 GW of demand from EV charging demand. As a result, the AC-OPF was solved, and there were no major voltage convergence issue. Figure 3.2 presents the voltage contour map of buses after including the effect of EVs with V2G discharging capacity. It is worth noting that this scenario assumes only 15% penetration of the overall cars in Texas with V2G capabilities.

*©2023 IEEE. Reprinted with permission from J.K. Jung et al., Spatiotemporal impact of electric vehicles in mitigating damages from destructive storms, *2023 IEEE Texas Power and Energy Conference*, February 2023

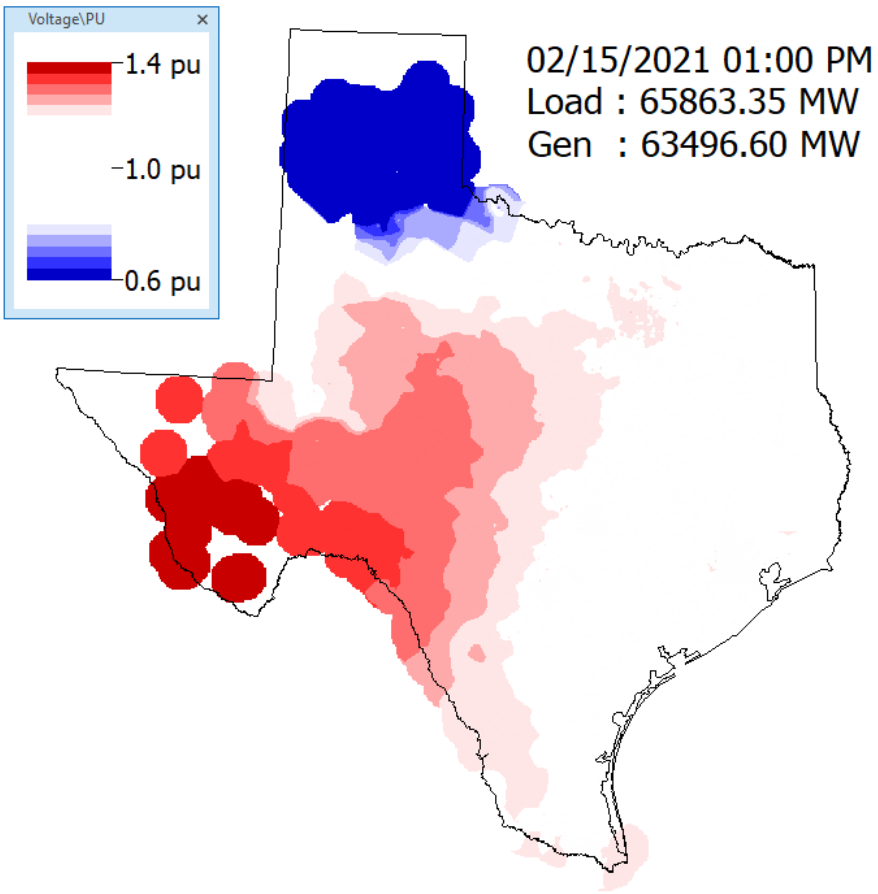

Figure 3.1: Voltage magnitude on February 15, 2021, with the base case. Reprinted with permission from [5].

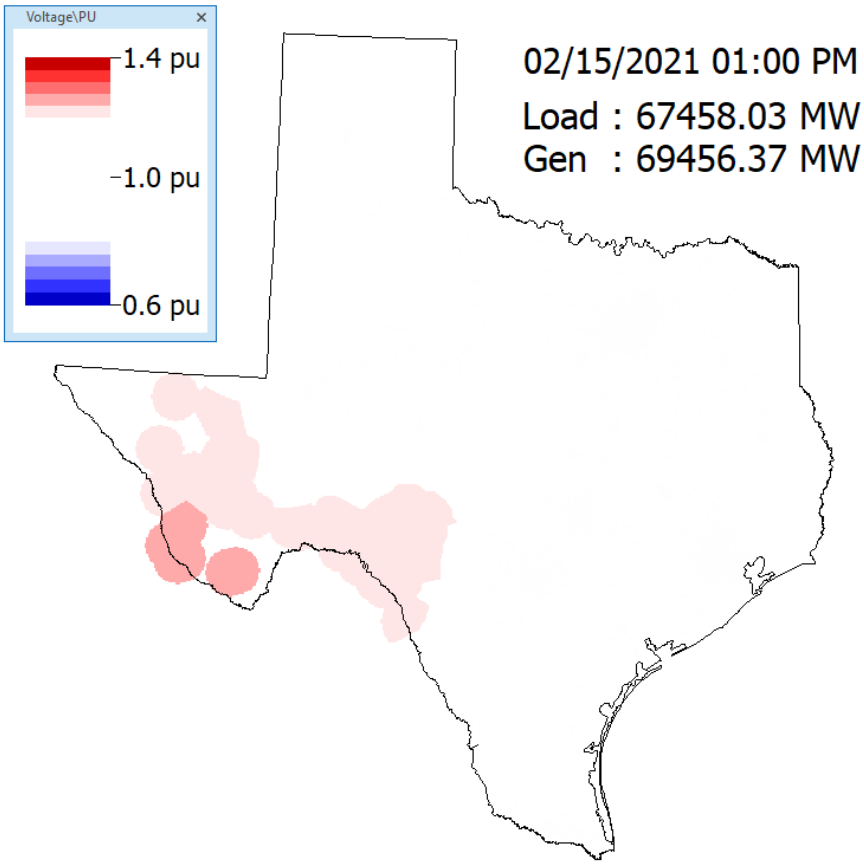

Figure 3.2: Voltage magnitude on February 15, 2021, with EV15% penetration. Reprinted with permission from [5].

4. CONCLUSION AND FUTURE WORK*

4.1 Conclusion

The study calculates the hourly demand required to charge EVs based on travel patterns and incorporates it into the hourly load of the Texas grid. The research investigates the potential use of EVs as a power source during severe weather events. To achieve this, the V2G discharging capabilities are added to the electrical grid when EVs are parked and in idle mode based on their end-of-travel coordinates and the short previous travel duration. The study assumes that 15% penetration of light-duty cars in two Texas cities, such as Austin and Houston are EVs with EV charging demand and discharging capabilities, and weather measurements, such as wind speed, cloud coverage, and temperatures, from a winter storm called Uri on February 15, 2021, in Texas, are included as input. Based on specific generator models, the capacities of generators and outputs of renewable generators are updated as output, and an AC-OPF is solved for a scenario with V2G technologies. Simulation results show that although the base case experiences a convergence issue and voltage collapse due to high load and less available generation, the addition of 15% penetration of EVs with V2 capabilities to the electrical grid overcomes these issues. These results demonstrate the potential advantage of utilizing EVs as a power source to enhance power grid stability and resilience during emergencies and the possibility of preventing losses of millions of dollars.

4.2 Future Work

This study plans to expand its research on the integration of EV charging demand and discharging capabilities in additional regions, in Dallas, and to include Austin and Houston in future simulations. To improve the realistic as well as accuracy of the simulations, the study aims to implement SCOPF in Powerworld to the next step of research. In addition, future studies will also consider the integration of medium- and heavy-duty EVs in the electrical grid in similar scenarios.

REFERENCES

[1] EIA, "U.S. electricity customers experienced eight hours of power interruptions in 2020." https://www.eia.gov/todayinenergy/detail.php?id=50316.

[2] ERCOT, "ERCOT Blackout 2021." https://energy.utexas.edu/sites/default/files/UTAustin%20%282021%29%20EventsFebruary2021TexasBlackout%2020210714.pdf/.

[3] NREL, "Utility scale battery storage." https://atb.nrel.gov/electricity/2022/utility-scale_battery_storage.

[4] Canalys, "Global car sales estimates." https://canalys.com/newsroom/canalys-global-electric-vehicle-sales-2020.

[5] J. K. Jung, F. Safdarian, J. L. Wert, D. Wallison, and T. J. Overbye, "Spatiotemporal impact of electric vehicles in mitigating damages from destructive storms," 2023.

[6] ERCOT, "2018 ercot system planning in texas." http://www.ercot.com/files/docs/2018/12/21/2018_LTSA_Report.pdf/.

[7] FERC, "NERC The report in region." https://www.naesb.org/pdf4/ferc_nerc_regional_entity_staff_report_Feb2021_cold_weather_outages_111621.pdf/.

[8] The White House, "Fact sheet: President biden announces steps to drive american leadership forward on clean cars and trucks." https://www.whitehouse.gov/briefing-room/statements-releases/2021/08/05/fact-sheet-president-biden-announces-steps-to-drive-american-leadership-forward-on-clean-cars-and-trucks/.

[9] DMV, "Vehicle titles and registration division." https://www.txdmv.gov/about-us: :text=Currently%2C%20there %20are%20more%20than%2022%20million%20registered%20vehicles%20in%20Texas.

[10] S. C. Johnson, D. J. Papageorgiou, M. R. Harper, J. D. Rhodes, K. Hanson, and M. E. Webber, "The economic and reliability impacts of grid-scale storage in a high penetration renewable energy system," *Advances in Applied Energy*, vol. 3, p. 100052, 2021.

[11] M. Yilmaz and P. T. Krein, "Review of the impact of vehicle-to-grid technologies on distribution systems and utility interfaces," *IEEE Transactions on Power Electronics*, vol. 28, no. 12, pp. 5673–5689, 2013.

[12] EPRI, "Open standards-based vehicle-to-grid: Value assessment, t. epri, palo alto, ca: 2019. 3002014771." https://www.epri.com/research/products/000000003002014771.

[13] F. Safdarian, L. Lamonte, A. Kargarian, and M. Farasat, "Distributed optimization-based hourly coordination for v2g and g2v," in *2019 IEEE Texas Power and Energy Conference (TPEC)*, pp. 1–6, IEEE, 2019.

[14] J. Dugan, S. Mohagheghi, and B. Kroposki, "Application of mobile energy storage for enhancing power grid resilience: A review," *Energies*, vol. 14, no. 20, p. 6476, 2021.

[15] M. Yilmaz and P. T. Krein, "Review of benefits and challenges of vehicle-to-grid technology," in *2012 IEEE Energy Conversion Congress and Exposition (ECCE)*, pp. 3082–3089, 2012.

[16] W. Wang, X. Fang, H. Cui, F. Li, Y. Liu, and T. J. Overbye, "Transmission-and-distribution dynamic co-simulation framework for distributed energy resource frequency response," *IEEE Transactions on Smart Grid*, vol. 13, no. 1, pp. 482–495, 2021.

[17] J. Geske and D. Schumann, "Willing to participate in vehicle-to-grid (v2g)? why not!," *Energy Policy*, vol. 120, pp. 392–401, 2018.

[18] Electrek.co, "Ford releases the unexpectedly affordable bi-directional residential charging system." https://electrek.co/2022/03/01/ford-launches-bi-directional-home-charging-station-surprisingly-good-price/: :text=Ford

[19] A. Wood, B. Wollenberg, and G. Sheblé, *Power Generation, Operation, and Control*. Wiley, 2013.

[20] M. F. Anjos, A. J. Conejo, *et al.*, "Unit commitment in electric energy systems," *Foundations and Trends® in Electric Energy Systems*, vol. 1, no. 4, pp. 220–310, 2017.

[21] K. Hara, M. Kimura, and N. Honda, "A method for planning economic unit commitment and maintenance of thermal power systems," *IEEE Transactions on Power Apparatus and Systems*, no. 5, pp. 427–436, 1966.

[22] R. Kerr, J. Scheidt, A. Fontanna, and J. Wiley, "Unit commitment," *IEEE Transactions on Power Apparatus and Systems*, no. 5, pp. 417–421, 1966.

[23] F. Safdarian, A. Mohammadi, and A. Kargarian, "Temporal decomposition for security-constrained unit commitment," *IEEE Transactions on Power Systems*, vol. 35, no. 3, pp. 1834–1845, 2019.

[24] D. Bienstock and A. Verma, "Strong np-hardness of ac power flows feasibility," *Operations Research Letters*, vol. 47, no. 6, pp. 494–501, 2019.

[25] K. Lehmann, A. Grastien, and P. Van Hentenryck, "Ac-feasibility on tree networks is np-hard," *IEEE Transactions on Power Systems*, vol. 31, no. 1, pp. 798–801, 2015.

[26] T. J. Overbye, F. Safdarian, W. Trinh, J. H. Yeo, Z. Mao, and J. Snodgrass, "An approach for the direct inclusion of weather information in the power flow," in *Hawaii International Conference on System Sciences (HICSS)*, 2023.

[27] U.S. Energy Information Administration, "United states eia-860." https://www.eia.gov/electricity/data/eia860/.

[28] J. L. Wert, K. S. Shetye, H. Li, J. H. Yeo, X. Xu, A. Meitiv, Y. Xu, and T. J. Overbye, "Coupled infrastructure simulation of electric grid and transportation networks," in *2021 IEEE Power & Energy Society Innovative Smart Grid Technologies Conference (ISGT)*, 2021.

[29] K. S. Shetye, H. Li, J. L. Wert, X. Xu, A. Meitiv, Y. Xu, and T. J. Overbye, "Generation Dispatch and Power Grid Emission Impacts of Transportation Electrification," in *2021 North American Power Symposium (NAPS)*, pp. 01–06, 2021.

[30] Texas A&M Transporation Institute, "The future of tdm." http://https://static.tti.tamu.edu/tti.tamu.edu/documents/PRC-15-25F.pdf/.

[31] SMU team, SMU Data Science Review: Vol. 5: No. 2, Article 8, "Urban traffic simulation: Network and demand representation impacts on congestion metrics." https://scholar.smu.edu/datasciencereview/vol5/iss2/8.

[32] C. Chan, B. Wang, J. Bachan, and J. Macfarlane, "Mobiliti: Scalable transportation simulation using high-performance parallel computing," in *2018 21st International Conference on Intelligent Transportation Systems (ITSC)*, pp. 634–641, 2018.

[33] X. Xu, H. A. Aziz, and R. Guensler, "A modal-based approach for estimating electric vehicle energy consumption in transportation networks," *Transportation Research Part D: Transport and Environment*, vol. 75, pp. 249–264, 2019.

[34] U.S. Department Of Energy, "Map & data - ev model sales in the united states." https://afdc.energy.gov/data/.

[35] J. L. Wert, K. S. Shetye, H. Li, J. H. Yeo, X. Xu, A. Meitiv, Y. Xu, and T. J. Overbye, "Coupled infrastructure simulation of electric grid and transportation networks," in *2021 IEEE Power & Energy Society Innovative Smart Grid Technologies Conference (ISGT)*, pp. 1–5, IEEE, 2021.

[36] H. Li, A. L. Bornsheuer, T. Xu, A. B. Birchfield, and T. J. Overbye, "Load modeling in synthetic electric grids," in *2018 IEEE Texas Power and Energy Conference (TPEC)*, pp. 1–6, IEEE, 2018.

[37] H. Li, J. H. Yeo, A. L. Bornsheuer, and T. J. Overbye, "The creation and validation of load time series for synthetic electric power systems," *IEEE Transactions on Power Systems*, vol. 36, no. 2, pp. 961–969, 2020.

[38] U.S. Census Bureau, "Zcta gazetteer file." https://www.census.gov/geographies/reference-files/time-series/geo/gazetteer-files.2019.htmllist-tab-WGX6046M8XT6UYUBXO.

[39] U.S. Energy Information Association, "U.s. energy information administration 860." http://https://www.eia.gov/electricity/data/eia860/.

[40] "A methodology for the creation of geographically realistic synthetic power flow models," in *2016 IEEE Power and Energy Conference at Illinois, PECI 2016*, 2016 IEEE Power and Energy Conference at Illinois, PECI 2016, (United States), Institute of Electrical and Electronics Engineers Inc., Apr. 2016.

[41] V. Krishnan, B. Bugbee, T. Elgindy, C. Mateo, P. Duenas, F. Postigo, J.-S. Lacroix, T. G. S. Roman, and B. Palmintier, "Validation of synthetic u.s. electric power distribution system data sets," *IEEE Transactions on Smart Grid*, vol. 11, no. 5, pp. 4477–4489, 2020.

[42] A. B. Birchfield, E. Schweitzer, M. H. Athari, T. Xu, T. J. Overbye, A. Scaglione, and Z. Wang, "A metric-based validation process to assess the realism of synthetic power grids," *Energies*, vol. 10, no. 8, 2017.

[43] Adam Birchfield, "Texas 7k synthetic grid." https://electricgrids.engr.tamu.edu/electric-grid-test-cases/datasets-for-arpa-e-perform-program/.

[44] T. J. Overbye, E. M. Rantanen, and S. Judd, "Electric power control center visualization using geographic data views," in *2007 iREP Symposium-Bulk Power System Dynamics and Control-VII. Revitalizing Operational Reliability*, pp. 1–8, IEEE, 2007.

[45] T. J. Overbye, J. L. Wert, K. S. Shetye, F. Safdarian, and A. B. Birchfield, "The use of geographic data views to help with wide-area electric grid situational awareness," in *2021 IEEE Texas Power and Energy Conference (TPEC)*, pp. 1–6, IEEE, 2021.

[46] DFW Clean Cities, "Texas electric vehicle mapping tool." https://www.dfwcleancities.org/evsintexas/.

[47] J. D. Weber and T. J. Overbye, "Voltage contours for power system visualization," *IEEE Transactions on Power Systems*, vol. 15, no. 1, pp. 404–409, 2000.